

ERDC/CRREL MP-21-21

Cold Regions Research and  
Engineering Laboratory



**US Army Corps  
of Engineers®**  
Engineer Research and  
Development Center



## **Photo-transformation of Aqueous Nitroguanidine and 3-nitro-1,2,4-triazol-5-one**

Emerging Munitions Compounds

Julie B. Becher, Samuel A. Beal, Susan Taylor,  
Katerina Dontsova, and Dean E. Wilcox

August 2021

**The U.S. Army Engineer Research and Development Center (ERDC)** solves the nation's toughest engineering and environmental challenges. ERDC develops innovative solutions in civil and military engineering, geospatial sciences, water resources, and environmental sciences for the Army, the Department of Defense, civilian agencies, and our nation's public good. Find out more at [www.erdclibrary.on.worldcat.org/discovery](http://www.erdclibrary.on.worldcat.org/discovery).

To search for other technical reports published by ERDC, visit the ERDC online library at <https://erdclibrary.on.worldcat.org/discovery>.

# **Photo-transformation of Aqueous Nitroguanidine and 3-nitro-1,2,4-triazol-5-one**

Emerging Munitions Compounds

Samuel A. Beal and Susan Taylor

*Cold Regions Research and Engineering Laboratory  
U.S. Army Engineer Research and Development Center  
72 Lyme Road  
Hanover, NH 03775*

Julie B. Becher and Dean E. Wilcox

*Department of Chemistry  
Dartmouth College  
Hanover, NH 03775*

Katerina Dontsova

*Department of Soil, Water, and Environmental Science  
University of Arizona  
Tucson, AZ 85721*

Final report

Approved for public release; distribution is unlimited.

Prepared for U.S. Army Corps of Engineers  
Washington, DC 20314

Under SERDP Project ER-2727

## Preface

This study was conducted for the U.S. Army Corps of Engineers (USACE) Funding for this work was received from the USACE Engineer Research and Development Center (ERDC) and from the Department of Defense (DoD) Strategic Environmental Research and Development Program (SERDP), Project ER-2727. Ms. Becher received additional support from several programs at Dartmouth College.

The work was performed by the Army's Engineer Research and Development Center, Cold Regions Research and Engineering Laboratory (ERDC-CRREL). At the time of publication of this paper, the Deputy Director of ERDC-CRREL Mr. David Ringelberg and the Director was Dr. Joseph Corriveau.

This article was originally published in *Chemosphere* on 22 April 2019.

The Commander of ERDC was COL Teresa A. Schlosser and the Director was Dr. David W. Pittman.

**DISCLAIMER:** The contents of this report are not to be used for advertising, publication, or promotional purposes. Citation of trade names does not constitute an official endorsement or approval of the use of such commercial products. All product names and trademarks cited are the property of their respective owners. The findings of this report are not to be construed as an official Department of the Army position unless so designated by other authorized documents.

**DESTROY THIS REPORT WHEN NO LONGER NEEDED. DO NOT RETURN IT TO THE ORIGINATOR.**

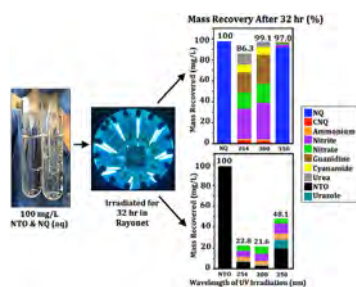
---

# Photo-transformation of aqueous nitroguanidine and 3-nitro-1,2,4-triazol-5-one: Emerging munitions compounds

---

## GRAPHICAL ABSTRACT

---



## ABSTRACT

---

Two major components of insensitive munition formulations, nitroguanidine (NQ) and 3-nitro-1,2,4-triazol-5-one (NTO), are highly water soluble and therefore likely to photo-transform while in solution in the environment. The ecotoxicities of NQ and NTO solutions are known to increase with UV exposure, but a detailed accounting of aqueous degradation rates, products, and pathways under different exposure wavelengths is currently lacking. Here, we irradiated aqueous solutions of NQ and NTO over a 32-h period at three ultraviolet wavelengths (254 nm, 300 nm, and 350 nm) and analyzed their degradation rates and transformation products. NQ was completely degraded by 30 min at 254 nm and by 4 h at 300 nm, but it was only 10% degraded after 32 h at 350 nm. Mass recoveries of NQ and its transformation products were  $\geq 80\%$  for all three wavelengths, and consisted of large amounts of guanidine, nitrate, and nitrite, and smaller amounts of cyanamide, cyanoguanidine, urea, and ammonium. NTO degradation was greatest at 300 nm with 3% remaining after 32 h, followed by 254 nm (7% remaining) and 350 nm (20% remaining). Mass recoveries of NTO and its transformation products were high for the first 8 h but decreased to 22–48% by 32 h, with the major aqueous products identified as ammonium, nitrate, nitrite, and a urazole intermediate. Environmental half-lives of NQ and NTO in pure water were estimated as 4 and 6 days, respectively. We propose photo-degradation pathways for NQ and NTO supported by observed and quantified degradation products and changes in solution pH.

---

## 1. Introduction

The U.S. military develops and tests insensitive munitions (IM) that are less sensitive to external stimuli and therefore less likely to

detonate unintentionally. Two IM formulations, IMX 101 and IMX 104, are current IM replacements for the high explosives 2,4,6-trinitrotoluene (TNT) and Composition B (1,3,5-trinitro-1,3,5-triazinane [RDX] and TNT), respectively. IMX 101 has already been approved by the U.S. Army as a safer, yet equally effective, alternative to TNT (Rutkowski et al., 2010). IMX 101 contains nitroguanidine (NQ), 3-nitro-1,2,4-triazol-5-one (NTO), and 2,4-dinitroanisole (DNAN), and IMX 104 contains NTO, DNAN, and RDX (S-Fig. 1). Both formulations are melt-cast, a process in which the crystalline components (i.e., NQ, NTO and RDX) are added to a molten DNAN matrix (Pelletier et al., 2010). Environmental releases of these compounds may occur as manufacturing wastewater or dispersal on soil as particles following detonations (Taylor et al., 2004; Hewitt et al., 2005; Jenkins et al., 2006; Walsh et al., 2013, 2014).

The water solubilities of NQ and NTO are orders of magnitude greater than their conventional counterparts at 4400 and 17000 mg/L, respectively (U.S. Army, 1984; Spear et al., 1989). Correspondingly, these compounds have been found to dissolve rapidly from IM particles upon surface exposure to water (Taylor et al., 2015a, 2015b). Complex biological and photochemical processes result in products that can have vastly different chemical properties than the starting explosives (Taylor et al., 2017a, 2017b; Halasz et al., 2018; Haag et al., 1990; Krzmarzick et al., 2015). Of particular concern is the noted increase in toxicity of NQ and NTO solutions when exposed to visible and ultraviolet light (van der Schalie, 1985; Kennedy et al., 2017; Gust et al., 2017). NTO and NQ absorb strongly at UV wavelengths (S-Fig. 2) making them susceptible to photochemical transformation by sunlight. The identification of photo-transformation rates, products, and pathways improves understanding of the fate, transport, and effects of IM releases.

Aqueous NQ irradiation experiments have found different photo-transformation products, some of which may explain its increased toxicity. Burrows et al. (1988) found guanidine, cyanoguanidine (CNQ), ammonia, nitrite, nitrate, urea and an intermediate (nitrosoguanidine) from 254 nm exposures. Haag et al. (1990a,b) found predominantly hydroxyguanidine and nitrites from sunlight exposures over four to six days. Halasz et al. (2018) found guanidine, nitrosoguanidine, and nitrates from a solar simulator (280–800 nm) and a 300 nm exposure. Although all of these compounds are more toxic than NQ (Burrows et al., 1988), Kennedy et al. (2017) posited that cyanide ( $\text{CN}^-$ ) might result from cyanamide or CNQ transformation. CNQ has been shown to breakdown into hydrogen cyanide under acidic conditions (NIOSH, 1998) and such a transformation would account for the drastic increase in solution toxicity (Kennedy et al., 2017).

Identified UV photo-transformation products of aqueous NTO include 3-hydroxy-1H-1,2,4-triazol-5(4H)-one, the tautomer of urazole, urazole, nitrates, triazolone, and carbon dioxide gas (Halasz et al., 2018; Singh et al., 2001; Le Champion et al., 1997). The reduced transformation product 3-amino-1,2,4-triazol-5-one (ATO) has been found from biotransformation under strictly anaerobic conditions but not photo-transformation of NTO (Le Champion et al., 1999a; Krzmarzick et al., 2015). In the presence of  $\text{TiO}_2$  or ferric salts, which catalyze Fenton chemistry, Le Champion et al. (1999b) demonstrated that NTO is entirely mineralized to carbon dioxide, ammonia and nitrate.

Transformation rates for NQ and NTO varied widely based on the irradiation wavelength and power used in the experiments (Halasz et al., 2018; Burrows et al., 1988; Haag et al., 1990; Kennedy et al., 2017). We aimed to understand the transformation pathways occurring in nature by establishing the NQ and NTO transformation rates at three different wavelengths and connecting these to sunlight exposure. To this end, we irradiated aqueous solutions of NQ

and NTO in a reactor chamber at UV-C, -B, and -A wavelengths to identify the photo-transformation products and rates at each UV wavelength. Although UV-C radiation is extremely low at the Earth's surface, the end products at this germicidal wavelength represent a sterile breakdown pathway. The identity of the photochemical transformation products of NQ and NTO and their rates of production are needed to determine their environmental impact.

## 2. Materials and methods

### 2.1. Experimental setup

NQ and NTO standards were obtained from BAE (97% pure). One liter bottles of 100 mg/L aqueous solutions of NQ and NTO were prepared using Milli-Q water. Eight mL of this stock solution were placed in quartz tubes and sealed with corks and parafilm. The samples were then placed in a rotating carousel in a Rayonet (RPR-100) reaction chamber (S-Fig. 3). Triplicate aqueous samples were irradiated for 0, 15 min, 30 min, 1 h, 2 h, 4 h, 8 h, 24 h, or 32 h at three different UV wavelengths. Eight bulbs at each wavelength had peak output at 254 nm, 300 nm, or 350 nm. The irradiation took place in a 4 °C cold room to counteract the heat produced by the bulbs. The inside of the irradiator had an average temperature of  $18.5 \pm 1.6$  °C minimizing thermal degradation of the samples. The pH of the samples was measured using a Mettler-Toledo pH meter and a micro pH probe, calibrated using pH 4, 7 and 10 standards.

### 2.2. Transformation product standards

Cyanoguanidine (99%), cyanamide (99%), urazole (97%), and guanidine hydrochloride ( $\geq 99\%$ ) standards were purchased from Sigma Aldrich. Urea (99%) was purchased from Bio-Rad. A standard of ATO was obtained from Ed Hunt (U. Arizona). Ammonium, nitrate, and nitrite ion chromatography (IC) standards were purchased in solution from Inorganic Ventures. All reagents for cyanide analysis were purchased from Sigma Aldrich. We were not able to obtain nitrosoguanidine and hydroxyguanidine standards.

### 2.3. Chromatography analyses

Aqueous samples were measured for NQ, cyanoguanidine, NTO, and urazole using a Hypercarb porous graphitic column ( $50 \times 2.1$  mm,  $3 \mu\text{m}$ ) on an Agilent 1200 HPLC with a diode array detector (modified from Le Champion et al., 1999a,b). For NQ, the mobile phase was 0.5% trifluoroacetic acid (TFA) in water from 0 to 10 min, 15/85 (v/v) acetonitrile/water with 0.1% TFA from 10 to 15 min, and 0.5% TFA in water from 15 to 19 min. For NTO, the mobile phase was 0.5% TFA from 0 to 5 min, 15/85 (v/v) acetonitrile/water with 0.1% TFA from 5 to 12 min, and 0.5% TFA in water from 12 to 17 min. The sample injection volume was 10  $\mu\text{L}$ , the flow rate was 0.4 mL/min, and the column temperature was 28 °C. Detection wavelengths and retention times were: 263 nm at 8.6 min for NQ; 216 nm at 2.8 min for CNQ; 315 nm at 9.6 min for NTO; and 216 nm at 3.0 min for urazole. The estimated detection limit for each analyte was 0.02 mg/L.

Aqueous NQ samples were analyzed for cyanamide and urea using a ProntoSIL 200-5-C30 column ( $250 \times 4.6$  mm,  $5 \mu\text{m}$ ) on an Agilent 1200 Series HPLC with a diode array detector (Turowski and Deshmukh, 2004). The mobile phase was 100% water at 0.8 mL/min and 28 °C. The total run time was 10 min and the injection volume was 20  $\mu\text{L}$ . The retention time was 3.9 min for cyanamide and 3.8 min for urea. This method also detected cyanoguanidine at 5.3 min and NQ at 6.6 min. The UV detector was set at 200 nm for all analytes. The estimated detection limit for each analyte was

0.02 mg/L.

Aliquots of each sample were diluted 1:10 and analyzed by ion chromatography with conductivity detection (Thermo Integrion). Ammonium and the guanidinium ion (reported as guanidine) were separated on an IonPac CS19 column (250 × 4 mm, 4 μm) with 7 mM methane sulfonic acid (Burrows et al., 1984). The flow rate was 1 mL/min, injection volume 25 μL, and column temperature 30 °C. Nitrate and nitrite were separated on an IonPac AS18 column (150 × 4 mm, 4 μm) with 25 mM KOH isocratic eluent. The estimated detection limit for each analyte was 0.2 mg/L.

#### 2.4. Cyanide analysis

We analyzed for HCN gas from the irradiated solutions using modified EPA methods 9010 for the scrubber solution and 9014 for the colorimetric analysis. A tiny test tube was suspended inside the quartz irradiation vials and filled with 0.5 mL of NaOH scrubber solution (5 g of NaOH in 100 mL of water). The scrubber solution should have absorbed any HCN gas evolved from the aqueous solutions of NQ and NTO. For the colorimetric analysis, a 1 M sodium phosphate solution, a 0.44% Chloramine-T solution, a pyridine-barbituric acid solution, and KI starch paper were used according to EPA method 9014 guidelines to measure HCN gas absorbed by the NaOH scrubber solution based on the solution absorbance at 578 nm (U.S. EPA, 2014).

#### 2.5. Irradiance measurements and rate calculations

Ultraviolet irradiance was measured in the reactor using an optometer (Gigahertz Optik P-9710). Three detector heads were used for the optometer corresponding to UV-A (Gigahertz Optik UV-3701; 315–400 nm), UV-B (UV-3702; 280–315 nm), and UV-C (UV-3703; 250–280 nm). Irradiance measurements were made inside the reactor at the location of the samples both in front of and between each bulb and averaged since the samples were rotating in the chamber. Assuming 100% transmission through the quartz tubes, we calculated fluence ( $J/m^2$ ) as the product of irradiance of a given detector head and irradiation time. We calculated first-order photolysis transformation rates ( $k_{obs}$ ) by the linear fit of the natural logarithm of normalized compound concentration and fluence (intercept forced through 0). Using the same detector heads, we measured irradiance at noon in Hanover, New Hampshire, United States (43.7 °N), on a clear day (7 May 2017) and a cloudy day (4 May 2017). We estimated environmental half-lives at each tested wavelength using  $k_{obs}$  and an estimate of daily fluence as half the clear day noon-measured irradiance over 8 h per day.

### 3. Results and discussion

#### 3.1. NQ transformation rates and products

All 101.5 mg/L of starting NQ was degraded by 30 min at 254 nm and by 4 h at 300 nm (Fig. 1). Approximately 92% of the original NQ remained after 32 h at 350 nm. The total mass recoveries of all measured compounds at the end of each 32-hr experiment were  $86 \pm 1\%$ ,  $99.1 \pm 0.9\%$ , and  $97.0 \pm 0.1\%$  for the 254 nm, 300 nm, and 350 nm bulb irradiations, respectively.

The rapid transformation of NQ from irradiation at 254 nm yielded relatively constant concentrations of guanidine, urea, cyanamide and CNQ (Fig. 1b). HCN gas was not detected in any of the irradiated solutions at 254 or 300 nm after 32 h exposure. Of the terminal aqueous nitrogen products, ammonium concentrations remained minimal throughout the experiment, while nitrate dominated from 15 min until after 8 h when a reversal occurred with nitrite becoming the predominant product. Solution pH

tracked the shift in  $NO_3^-/NO_2^-$  with an initial decrease followed by a return to neutral pH by 24 h.

At 300 nm, the slower transformation of NQ yielded fairly constant relative abundances of nitrite, guanidine, nitrate, cyanamide, urea, and CNQ (Fig. 1c). The 300 nm irradiation produced greater guanidine concentrations and lesser urea concentrations, compared with the 254 nm irradiation. Nitrite concentrations were greater than nitrate throughout the irradiation, but longer irradiation times increased nitrate at the expense of nitrite, which was reflected in the solution pH that decreased throughout the experiment. Interestingly, after 30 min more oxygen was recovered than was in the initial NQ (S-Fig. 4), likely due to the oxidation of ammonia to nitrate, which has been observed under UV irradiation of  $pH \geq 7$  solutions when hydroxyl radicals are present (Huang et al., 2008). Photoreactions of nitrate and nitrite can create the hydroxyl radicals necessary for ammonia oxidation (Mack and Bolton, 1999), and the pH of the 300 nm solutions was high enough to enable this process. This positive oxygen mass balance was not observed for irradiation at 254 nm, likely because its relatively acidic pH inhibited ammonia oxidation, which in turn may partially explain the negative nitrogen mass balance in those samples as loss of ammonia gas. The additional oxygen in the 300 nm samples artificially increased the total percent mass recoveries by ~6%.

After 32 h of 350 nm irradiation, NQ concentrations were  $93.6 \pm 0.1$  mg/L with ~1–3 mg/L each of nitrate, nitrite, ammonium, and guanidine, and no detectable CNQ or urea. The pH of these solutions was constant during irradiation, indicating that a change in pH is related to NQ breakdown. Slow transformation at 350 nm likely reflects NQ's relatively low photon absorption at this wavelength ( $\lambda_{max}$  264 nm, S-Fig. 2).

An unknown peak was observed in the HPLC analyses of the 254 and 300 nm samples. On the Hypercarb column the unknown compound had a retention time of 2.44–2.56 min and an absorbance peak at 240 nm (Fig. 2). On the ProntoSIL column the unknown peak was observed at 4.48 min with an absorbance maximum at 258 nm. We attribute the 18 nm shift in the maximum to differences in the mobile phase solution, and suggest these peaks correspond to the same unknown.

The unknown was transient, increasing in concentration as NQ concentrations decreased, and then steadily decreasing in concentration until it disappeared around 8 h for the 254 nm samples. The timing of the unknown's appearance and disappearance is consistent with nitrosoguanidine found by Burrows et al. (1988). For the first 4 h of irradiation, not all of the nitro groups from NQ decomposition were recovered as nitrate and nitrite. By 8 h, however, all of the nitro group mass was detected as these two ions. The concentration of guanidine also did not peak until 2 h in the 254 nm irradiated samples, yet NQ was fully degraded after 30 min. This suggests that a portion of the nitro groups and guanidine initially existed in an intermediate compound but was transformed into guanidine and nitrates with longer UV exposure. The nitrosoguanidine intermediate observed by Burrows et al. (1988) follows this same behavior. Furthermore, Burrows et al. (1988) observed nitrosoguanidine to absorb radiation strongly at 235 nm, which is close to the absorbance peak of the unknown intermediate (240–258 nm).

#### 3.2. NQ photo-transformation pathways

The weakest bond in NQ is the N–NO<sub>2</sub> bond with a dissociation energy of 199.1 kJ/mol (Xue et al., 2017). When the N–NO<sub>2</sub> bond is photolytically cleaved, NQ separates into the guanidine radical and nitro radical. The guanidine radical can form guanidine by abstraction of a hydrogen atom from the solution, form

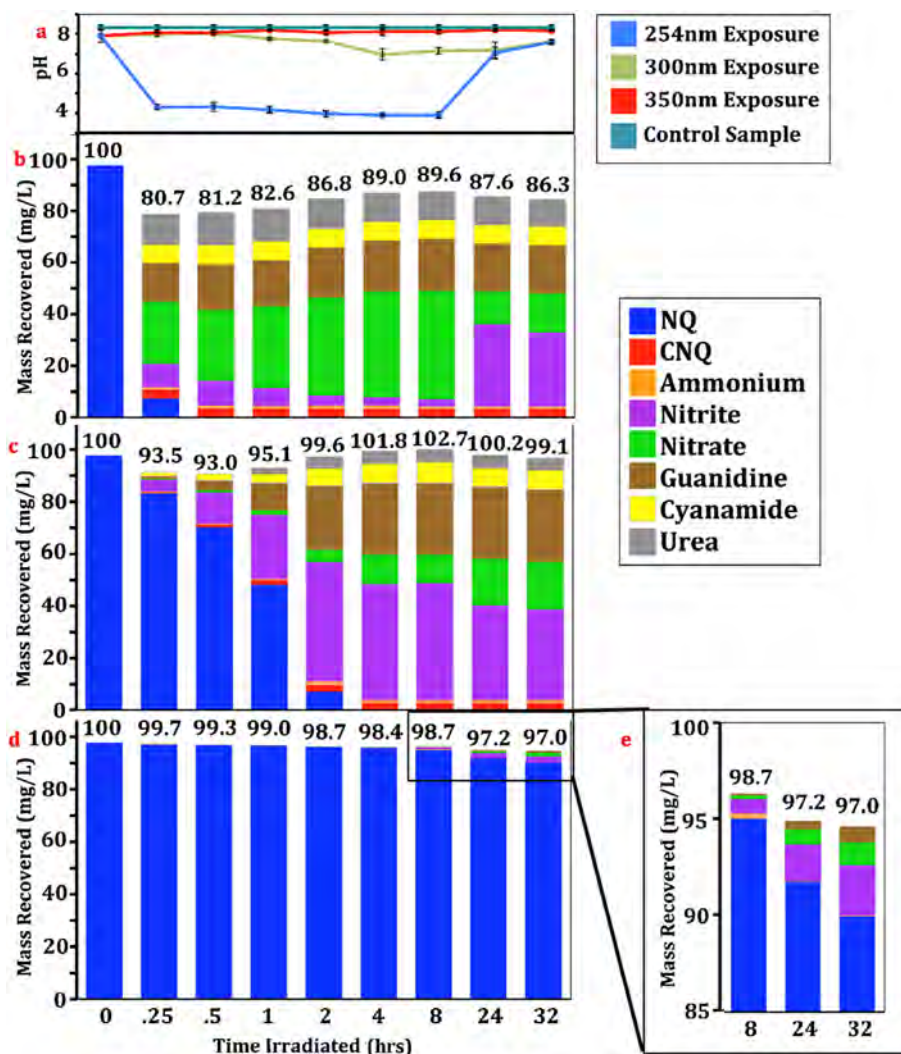


**Fig. 1.** NQ sample pH (a.) and chemical concentrations at 254 nm irradiation (b.), 300 nm irradiation (c.), and 350 nm irradiation (d. and e.). pH error bars are  $\pm 1$  standard deviation. Bars reflect the mean concentration of each compound from triplicate samples. The mass percentages recovered for each time step are shown above each bar.

hydroxyguanidine by reacting with water, or breakdown into ammonia and cyanamide (intramolecular collapse). The latter can then dimerize into CNQ or be hydrolyzed to urea (Fig. 3). The nitro radical either gains one electron and becomes nitrite or is oxidized further to become nitrate. Although we had no standard for hydroxyguanidine, our high mass recoveries make its existence in large quantities unlikely. Burrows et al. (1988) proposed an alternative pathway to produce the nitrosoguanidine intermediate—the disproportionation of NQ into nitrosoguanidine and an oxidized intermediate. Our data suggest that this pathway is minor compared to the homolytic cleavage of the N–N bond, since very little of the nitro and guanidine mass came from this intermediate.

Under 254 nm irradiation, over half of the carbon from the guanidine portion of the molecule was recovered as cyanamide, urea, and CNQ, indicating that intramolecular collapse of the guanidine radical is a major pathway at this wavelength. Cyanamide persisted in solution in significant amounts ( $\sim 8$  mg/L), with preferential hydrolysis into urea, rather than dimerization into CNQ. Cyanamide formed when the samples were acidic ( $\sim$ pH 4), which favors the reaction toward urea, while the reaction toward CNQ is favored at a pH  $> 5$  (Urbanyi and Walter, 1971).

More guanidine was formed with 300 nm irradiation, compared to 254 nm irradiation, and there was less cyanamide, suggesting

that higher energy is needed to collapse the guanidine radical. Correspondingly lower concentrations of urea and CNQ were observed at 300 nm. Although more of the guanidine carbon was recovered as guanidine than as intramolecular collapse products (cyanamide, urea, CNQ), more of the carbon recovered from intramolecular collapse remained as cyanamide than was converted to either CNQ or urea. This finding differs from the predictions of Burrows et al. (1988) who suggested that cyanamide was an unstable intermediate in the breakdown pathway, rather than an end-stage transformation product, as we found. Under 350 nm irradiation, no CNQ, cyanamide or urea were detected, but some guanidine was found, suggesting that homolytic cleavage of the N–NO<sub>2</sub> bond is not favored and intramolecular guanidine radical collapse is not a viable pathway at this wavelength.

Rapid breakdown of NQ from homolytic cleavage of the N–NO<sub>2</sub> bond likely forms many nitro radicals, which dimerize into N<sub>2</sub>O<sub>4</sub>, an intermediate in the photoreaction pathway that transforms nitrite into nitrate (S-Fig. 5; Mack and Bolton, 1999). Protons are liberated by this transformation in water, which accounts for the initial pH drop observed for the 254 nm solutions. Low pH inhibits the photoreactions that convert nitrate to nitrite (Mack and Bolton, 1999), leading to high nitrate concentrations during the early stages of the exposure period. Once NQ was fully degraded and nitro radicals



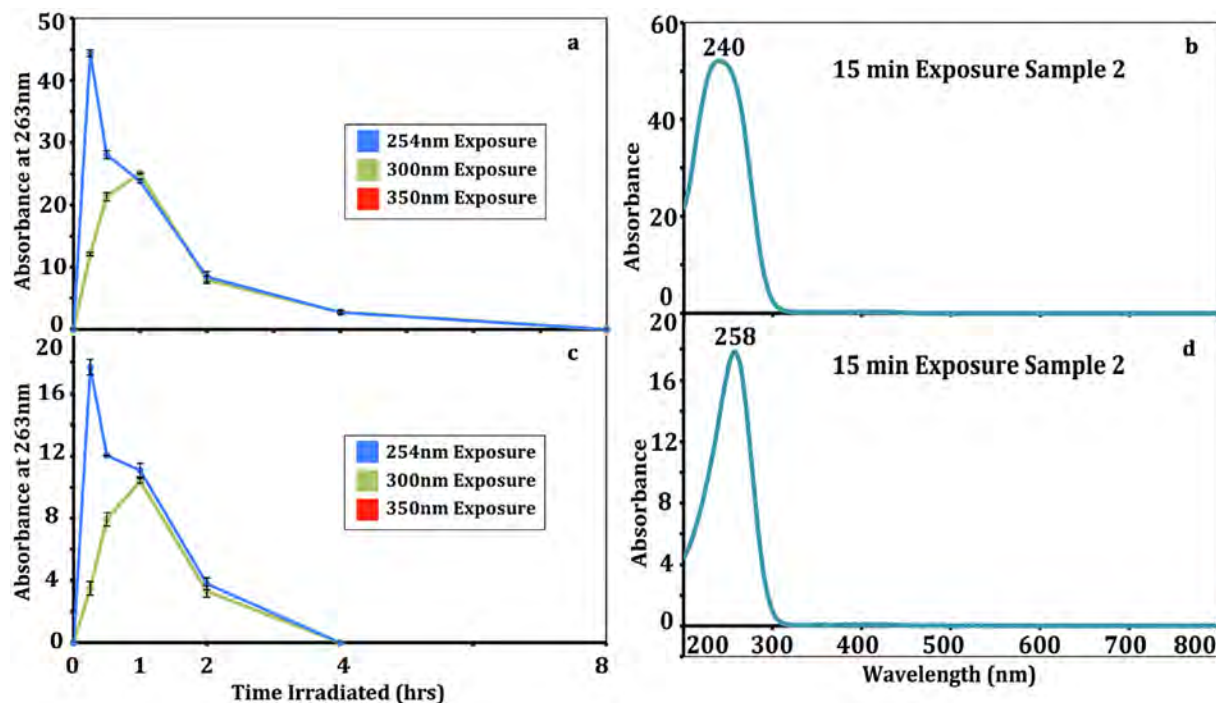


Fig. 2. HPLC absorbance and DAD spectra of the NQ irradiation unknown, suspected to be nitrosoguanidine, using a Hypercarb column (a–b) and ProntoSIL column (c–d).

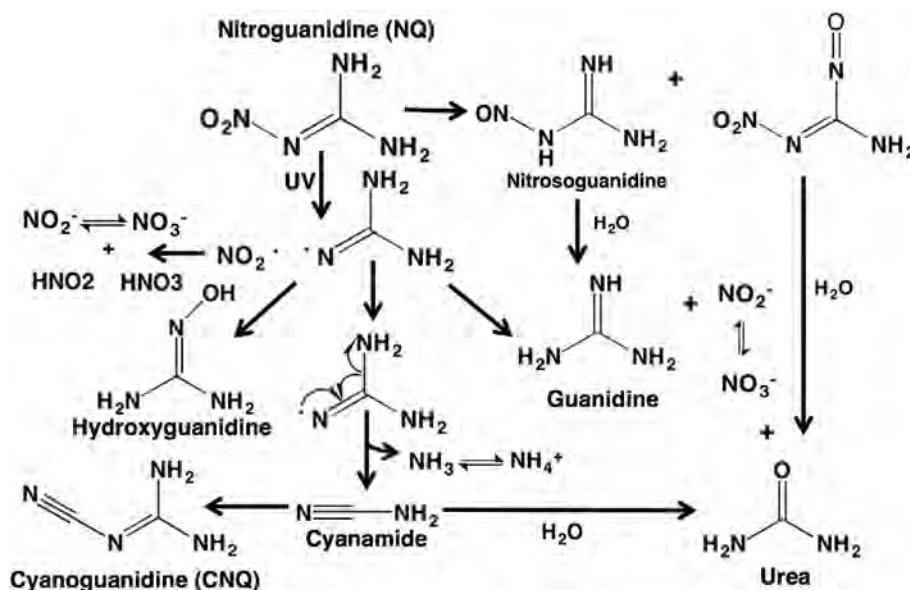


Fig. 3. Breakdown pathways of nitroguanidine (NQ) under UV irradiation. Major predicted transformation products are labeled. Adapted from Burrows et al., (1988) and Haag et al., (1990).

were no longer generated, photoreactions transforming nitrate into nitrite lead to intermediates ( $\cdot\text{OH}$ ,  $\text{O}_2^{\cdot-}$ ) that scavenged protons from solution, thereby increasing the solution pH. This same process likely occurred in all of the irradiated solutions but the kinetics varied based on the wavelength of irradiation and rate of NQ transformation.

Our results show that cyanamide, urea and CNQ (in small amounts) are the final transformation products, and not intermediates, of NQ photo-transformation. The amounts of nitrate and nitrite produced vary depending on the time of exposure and

the UV wavelength used, but are produced in large amounts that could have harmful environmental effects. Nitrates are quite toxic to aquatic life (Camargo et al., 2005) and nitrite is a potential carcinogen, due to the formation of N-nitrosamine compounds in the stomach, when consumed by humans (Mirvish, 1975). While cyanide would explain the extreme toxicity of irradiated NQ solutions, we did not detect HCN vapor above the irradiated solutions. Possibly a more sensitive cyanide detection method is required. In the presence of the weak acid NTO, as would occur from IMX-101 dissolution in the environment, CNQ could be transformed into

extremely toxic HCN.

### 3.3. NTO rates and products

After 32 h of irradiation at 254 nm, 300 nm, and 350 nm, only 7%, 3%, and 20% of the initial NTO remained, respectively (Fig. 3). The mass recovery of these samples was initially high (74–101%) but decreased dramatically after 8 h and was quite low by 32 h of irradiation ( $22.8 \pm 2.8\%$ ,  $21.6 \pm 0.5\%$ , and  $48.1 \pm 0.7\%$  for 254 nm, 300 nm, and 350 nm, respectively; Fig. 4). The final transformation products from NTO irradiation at all three wavelengths were ammonium, nitrate, and nitrite, with urazole appearing transiently. Formation of bubbles in irradiated NTO solutions (S-Fig. 6) suggests gaseous transformation products that were not quantified and may explain the poor mass recoveries. Interestingly, the highest amounts of ammonium, nitrate, nitrite, unknown anion, and

urazole per mg of degraded NTO were observed in the 350 nm samples, even though NTO breakdown was slowest at this wavelength.

Nitrite increased before reaching stable concentrations by 8 h in the 254 and 300 nm samples and by 24 h in the 350 nm samples. Nitrate and ammonium concentrations increased at all three wavelengths throughout the experiment. Nitrite and nitrate concentrations in the NTO samples were significantly lower, and ammonium significantly higher, than those produced by irradiation of NQ. Urazole concentrations increased linearly until a maximum of ~12 mg/L was detected at 8 h in the 254 nm and 300 nm samples, and at 24 h in the 350 nm samples, before linearly decreasing until 32 h. An unknown anion that formed transiently, similarly to urazole, was identified by ion chromatography in 254 nm and 300 nm samples but persisted throughout the experiment at 350 nm (Fig. 5, S-Fig. 7). Cyanate was rejected as the identity of the unknown

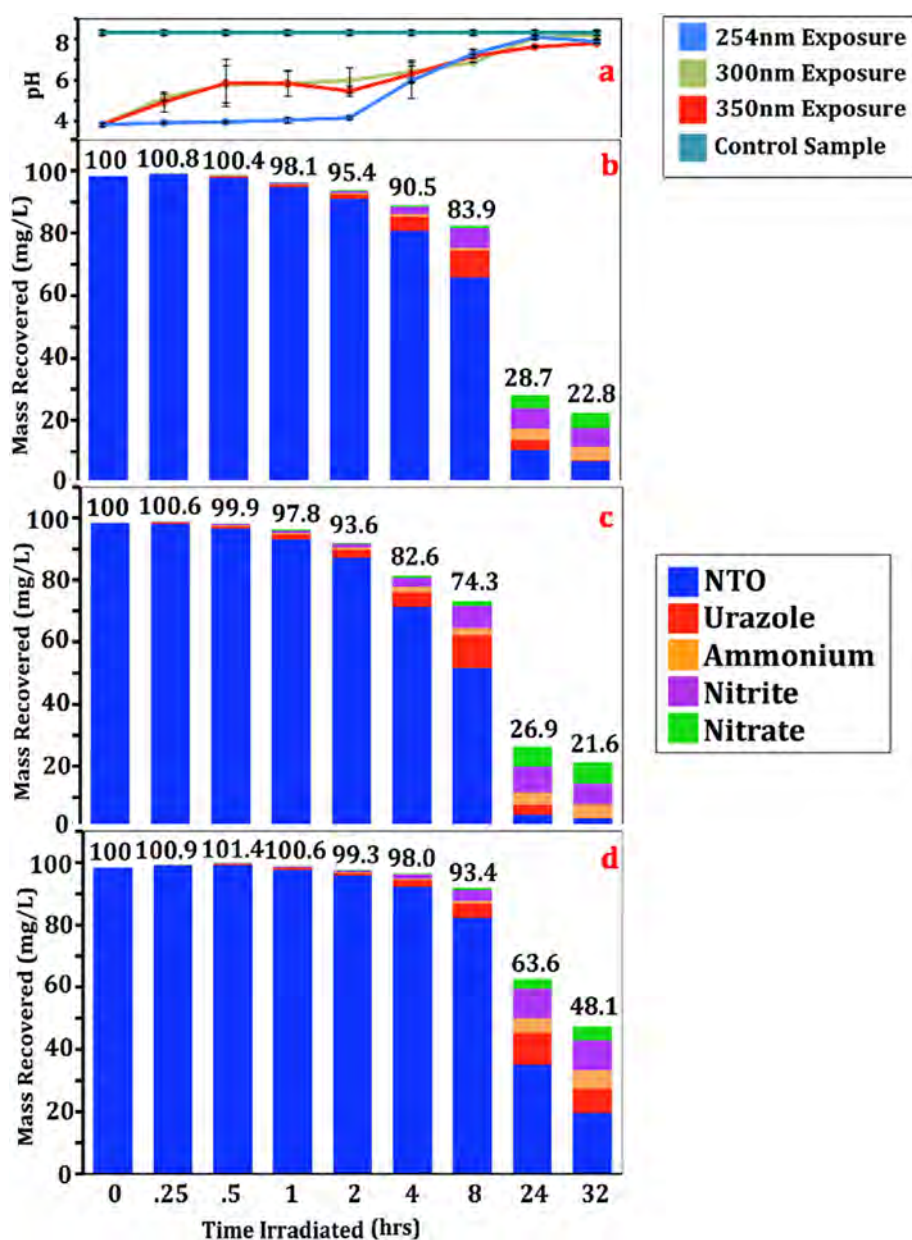


Fig. 4. NTO sample pH (a.) and chemical concentrations at 254 nm irradiation (b.), 300 nm irradiation (c.), and 350 nm irradiation (d.). pH error bars are  $\pm 1 \sigma$ . Bars reflect the mean concentration of each compound from triplicate samples. The mass percentages recovered for each time step are shown above each bar.

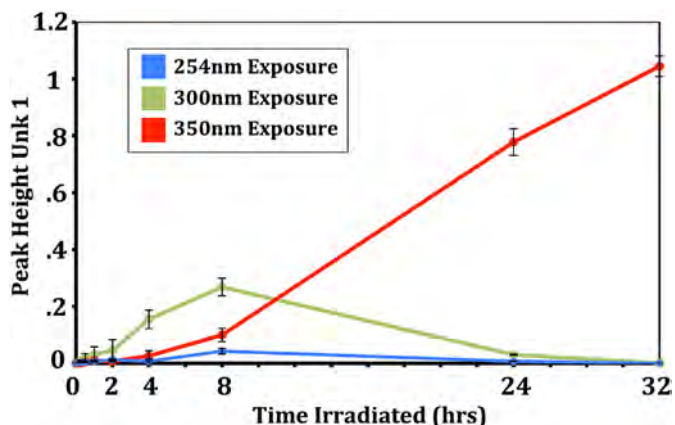


Fig. 5. Peak height of an unknown in the anion IC chromatograms for NTO. Error bars are  $\pm 1\sigma$  of triplicate samples at each wavelength.

intermediate, based on analysis of a known standard. The pH of these samples was initially acidic because of NTO's  $pK_a$  of 3.76 (Smith and Cliff, 1999) but increased over the course of the experiment and reached neutral values.

### 3.4. Transformation pathways for NTO

The NTO solutions were initially yellow, but became clear when irradiated, indicating ring cleavage or a loss of aromaticity. For NTO, the C–NO<sub>2</sub> bond is weakest with a dissociation energy of 281 kJ/mol (Hadisaputra and Prasetyo, 2016). Breaking this bond results in a nitro radical and a triazolone radical, which reacts with water to form urazole, the major intermediate product of NTO (Singh et al., 2001; Halasz et al., 2018).

We propose that ring hydrolysis of either urazole or NTO directly forms an intermediate that can break down into isocyanic acid or other derivatives (Fig. 6). These derivatives are further hydrolyzed into the volatile products ammonia and carbon dioxide (Borduas et al., 2016). This pathway is analogous to that proposed for ATO, which forms cyanamide in soil before being mineralized

further (FAO, 1999). The proposed pathway explains both the presence of ammonium and the gas bubbles we observed (S-Fig. 6). We found urazole but the other potential intermediates (hydrazine, (hydrazinocarbonyl)-carbamic acid) would need to be detected and identified to confirm the proposed pathway. The unknown anion found in the NTO samples may be an intermediate in this breakdown pathway.

Since the NTO transformation products were found in approximately equal ratios and amounts at all three wavelengths, the NTO transformation pathway does not depend on the wavelength of irradiation. The wavelength does, however, determine the rate at which the NTO degrades. NTO should photo-transform most quickly at 350 nm, the wavelength closest to its absorbance peak. Interestingly, NTO photo-transformed most quickly at 300 nm (Fig. 3), suggesting that other species affected its transformation rate rather than direct photolysis. These species could include ozone, possibly singlet oxygen species, or other reactive oxygen species created as nitrite and nitrate build up in solution.

The low mass recovery for the irradiated NTO solutions was likely due to both unidentified transformation products and the mass loss from gaseous products, as indicated by gas bubbles in the irradiated NTO solutions (S-Fig. 6). Based on the mass of transformed NTO, if we assume full mineralization of the missing C mass as CO<sub>2</sub>, and the missing ring N as NH<sub>3</sub>, as observed by Le Campion et al. (1999b), ~63 mg of CO<sub>2</sub> and 39 mg of NH<sub>3</sub> could have been produced per liter of our 99.8 mg/L NTO solution during the 32-h experiment at 254 nm, 65 mg CO<sub>2</sub> and 51 mg NH<sub>3</sub> at 300 nm, and 54 mg CO<sub>2</sub> and 42 mg NH<sub>3</sub> at 350 nm.

### 3.5. Environmental transformation rates

The amount of UV and visible light that reaches the Earth's surface varies as a function of many parameters, including latitude, time of year, and atmospheric and weather conditions (Brennan and Fedor, 1994). Although neither direct nor indirect photolysis guidelines (i.e., U.S. EPA OPPTS 835.5270 and 835.2210) were followed in this study due to our focus on mechanisms at individual UV wavelengths, we estimated environmental half-lives of NTO and NQ in pure water. We applied the fluence-based first-order transformation rates from the reactor experiments to measurements of

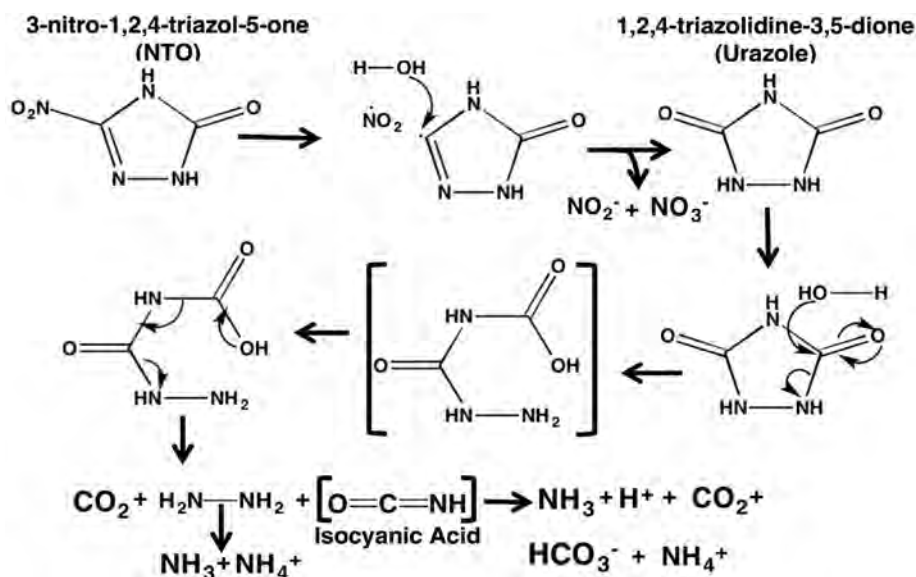


Fig. 6. Breakdown pathways of NTO under UV irradiation. Major predicted transformation products are labeled. Adapted from Halasz et al., (2018), FAO and WHO, 1999, Singh et al., (2001), and Borduas et al., (2016).

**Table 1**  
First-order photo-transformation rates and estimated environmental half-lives based on measured sunlight irradiance (S-Table 2).

Irradiation Wavelength	NQ $k_{\text{obs}}$ ( $\text{m}^2/\text{J} \pm 1\text{SE}$ )	NTO $k_{\text{obs}}$ ( $\text{m}^2/\text{J} \pm 1\text{SE}$ )	NQ est. $t_{1/2, \text{env}}$ (days)	NTO est. $t_{1/2, \text{env}}$ (days)
254 nm	$-3.75 \pm 0.02 \times 10^{-5}$	$-2.9 \pm 0.1 \times 10^{-7}$	68	8700
300 nm	$-7.2 \pm 0.9 \times 10^{-6}$	$-7.2 \pm 0.3 \times 10^{-7}$	4	41
350 nm	$-7.8 \pm 0.6 \times 10^{-9}$	$-1.70 \pm 0.09 \times 10^{-7}$	130	6

outdoor surface UV irradiance (S-Table 2) at each UV band in order to estimate the environmental half-lives (Table 1, S-Fig. 8). In sunlight, NQ is estimated to degrade most rapidly by 300 nm (UV-B) light with a half-life of ~4 days. NTO is estimated to degrade most rapidly by 350 nm (UV-A) light with a half-life of ~6 days. The estimated NQ half-life has a similar order-of-magnitude to that determined in aqueous solutions by outdoor photolysis (0.68–0.70 days; Haag et al., 1990a,b) and by solar simulator (0.59 days; Halasz et al., 2018). The estimated NTO half-life also has a similar order-of-magnitude to that determined in aqueous solution by solar simulator (2.0 days; Halasz et al., 2018). These environmental half-lives by sunlight are comparable to those for RDX (0.8–2.5 days), nitroglycerin (26–123 days), and DNAN (2.6 days) dissolved in pure water (Bordeleau et al., 2013; Halasz et al., 2018). In natural waters, however, quenching or indirect photolysis of NQ and NTO by dissolved species (e.g., dissolved organic matter, other energetic compounds) may affect photo-transformation rates and products (Haag et al., 1990; Dontsova et al., 1984; Halasz et al., 2018).

#### 4. Conclusions and environmental implications

NQ and NTO are likely to undergo photo-transformation in wastewater or in surface water impacted by post-detonation particles with half-lives on the order of days. Increased toxicity of photo-transformed NQ may result from the formation of the terminal products cyanamide, CNQ, guanidine, and/or high levels of nitrate and nitrite, or from the transient formation of nitrosoguanidine. Further studies on these transformation compounds, particularly guanidine and nitrosoguanidine, could reveal the mechanism of irradiated NQ's toxicity. Additionally, although HCN gas was not observed during the irradiations, concentrations may have been below the method detection limit yet still significantly toxic, requiring a more sensitive detection method in future work. Irradiation of NTO solutions has been shown to slightly increase its eco-toxicity, but this study's irradiations produced predominantly mineralized gases, moderate nitrate and nitrite concentrations, and minimal amounts of the transient compound urazole, the latter of which has unknown toxicity. Since both NTO and NQ are present in the IMX 101 formulation, these compounds are probably found in the same surface water and may interact to promote or inhibit certain transformation pathways. For instance, the weak acid NTO could favor the transformation of photo-produced CNQ into extremely toxic HCN. Irradiation experiments of complete formulations (IMX 101 and 104) in natural waters are needed to confirm these results and enable environmental efforts to focus on transformation products that are both toxic and persistent in the environment.

#### Acknowledgements

We thank Marianne Walsh, David Ringelberg, and Karen Foley at CRREL and Jean Carlan at Dartmouth for laboratory assistance. Funding for this work was received from the US Army Engineer Research and Development Center and from the Strategic Environmental Research and Development Program project ER 2727. JB received additional support from the Women in Science Program,

the Sophomore Science Scholars Program, the James O. Freedman Presidential Scholars Program and the John L. Zabriskie Jr. 1961 Fund in Chemistry at Dartmouth College.

#### Appendix A. Supplementary data

Supplementary data to this article can be found online at <https://doi.org/10.1016/j.chemosphere.2019.04.131>.

#### References

- Army, U.S., 1984. Military Explosives. Technical Manual TM 9-1300-214. Method 9010C: Total and Amenable Cyanide: Distillation; Test Methods for Evaluating Solid Waste: Physical/Chemical Methods; EPA Method SW-846 Update V, 2004. U.S. Environmental Protection Agency. Available online at: <https://www.epa.gov/sites/production/files/2015-03/documents/9546041.pdf>.
- Bordeleau, G., Martel, R., Ampleman, G., Thiboutot, S., 2013. Photolysis of RDX and nitroglycerin in the context of military training ranges. *Chemosphere* 93, 14–19.
- Borduas, N., Place, B., Wentworth, G.R., Abbott, J.P.D., Murphy, J.G., 2016. Solubility and reactivity of HNCO in water: insights into HNCO's fate in the atmosphere. *Atmos. Chem. Phys.* 16 (2), 703–714.
- Brennan, P., Fedor, C., 1994. Sunlight, UV, and Accelerated Weathering; Technical Bulletin LU-0822. Q-Panel Company, Cleveland, OH.
- Burrows, E.P., Brueggeman, E.E., Hoke, S.H., 1984. Chromatographic trace analysis of guanidine, substituted guanidines and S-triazines in water. *J. Chromatogr. A* 294, 494–498.
- Burrows, W.D., Schmidt, M.O., Chyrek, R.H., Noss, C.I., 1988. Photochemistry of Aqueous Nitroguanidine. Technical Report 8808. U.S. Army BRDL: Fort Detrick, Frederick, MD.
- Camargo, J.A., Alonso, A., Salamanca, A., 2005. Nitrate toxicity to aquatic animals: a review with New data for freshwater invertebrates. *Chemosphere* 58 (9), 1255–1267.
- Le Campion, L., Adeline, M.T., Ouazzani, J., 1997. Separation of NTO related 1,2,4-triazole-3-one derivatives by a high performance liquid chromatography and capillary electrophoresis. *Propellants, Explos. Pyrotech.* 22 (4), 233–237.
- Le Campion, L., Giannotti, C., Ouazzani, J., 1999a. Photocatalytic degradation of 5-nitro-1,2,4-triazol-3-one NTO in aqueous suspension of TiO<sub>2</sub>. Comparison with Fenton oxidation. *Chemosphere* 38 (7), 1561–1570.
- Le Campion, L., Vandais, A., Ouazzani, J., 1999b. Microbial remediation of NTO in Aqueous Industrial wastes. *FEMS Microbiol. Lett.* 176 (1), 197–203.
- NIOSH, 1998. Dicyandiamide; ICSC No. 0650 (U.S. National Version). National Institute for Occupational Safety and Health, Centers for Disease Control and Prevention, Atlanta, GA [Online].
- Dontsova, K., Taylor, S., Pesce-Rodriguez, R., Brusseau, M., Arthur, J., Mark, N., Walsh, M., Lever, J., Šimůnek, J., 1984. Dissolution of NTO, DNAN, and Insensitive Munitions Formulations and Their Fates in Soils: Dissolution of NTO, DNAN, and Insensitive Munitions Formulations and Their Fates in Soils. Technical Report TR-14-23. Cold Regions Research and Engineering Laboratory, Hanover, NH.
- FAO (Food and Agriculture Organization of the United Nations) and WHO (World Health Organization), 1999. Amitrole (079) in Pesticide Residues in Food: 1998. Report of the Joint Meeting of the FAO Panel of Experts on Pesticides Residues in Food and the Environment and the WHO Core Assessment Group on Pesticide Residues. Food and Agriculture Organization of the United Nations, Rome, pp. 30–56. Rome, Italy, 21–30 September 1998. <http://www.who.int/iris/handle/10665/42262>.
- Gust, K.A., Stanley, J.K., Wilbanks, M.S., Mayo, M.L., Chappell, P., Jordan, S.M., Moores, L.C., Kennedy, A.J., Barker, N.D., 2017. The increased toxicity of UV-degraded nitroguanidine and IMX-101 to zebrafish larvae: evidence implicating oxidative stress. *Aquat. Toxicol.* 190, 228–245.
- Haag, W.R., Spanggard, R., Mill, T., Podoll, R.T., Chou, T.-W., Tse, D.S., Harper, J.C., 1990a. Aquatic environmental fate of nitroguanidine. *Environ. Toxicol. Chem.* 9 (11), 1359–1367.
- Haag, W.R., Spanggard, R., Mill, T., Podoll, R.T., Chou, T.-W., Tse, D.S., Harper, J.C., 1990b. Aquatic environmental fate of nitroguanidine. *Environ. Toxicol. Chem.* 9, 1359–1367.
- Hadisaputra, S., Prasetyo, N., 2016. The explosive sensitivity on the complex formation of 3-nitro-1,2,4-triazol-5-one and metal ions based on density functional study. *Makara J. Sci.* 81–87–87.
- Halasz, A., Hawari, J., Perreault, N.N., 2018. New insights into the photochemical degradation of the insensitive munition formulation IMX-101 in water. *Environ. Sci. Technol.* 52 (2), 589–596.

- Hewitt, A.D., Jenkins, T.F., Walsh, M.E., Walsh, M.R., Taylor, S., 2005. RDX and TNT residues from live-fire and blow-in-place detonations. *Chemosphere* 61, 888–894.
- Huang, L., Li, L., Dong, W., Liu, Y., Hou, H., 2008. Removal of ammonia by OH radical in aqueous phase. *Environ. Sci. Technol.* 42 (21), 8070–8075.
- Jenkins, T.F., Hewitt, A.D., Grant, C.L., Thiboutot, S., Ampleman, G., Walsh, M.E., Ranney, T.A., Ramsey, C.A., Palazzo, A.J., Pennington, J.C., 2006. Identity and distribution of residues of energetic compounds at army live-fire training ranges. *Chemosphere* 63, 1280–1290.
- Kennedy, A.J., Poda, A.R., Melby, N.L., Moores, L.C., Jordan, S.M., Gust, K.A., Bednar, A.J., 2017. Aquatic toxicity of photo-degraded insensitive munition 101 (IMX-101) constituents. *Environ. Toxicol. Chem.* 36 (8), 2050–2057.
- Krzmarzick, M.J., Khatiwada, R., Olivares, C.I., Abrell, L., Sierra-Alvarez, R., Chorover, J., Field, J.A., 2015. Biotransformation and degradation of the insensitive munitions compound, 3-nitro-1,2,4-triazol-5-one, by soil bacterial communities. *Environ. Sci. Technol.* 49 (9), 5681–5688.
- Mack, J., Bolton, J.R., 1999. Photochemistry of nitrite and nitrate in aqueous solution: a review. *J. Photochem. Photobiol. A Chem.* 128 (1), 1–13.
- Mirvish, S.S., 1975. Formation of N-nitroso compounds: chemistry, kinetics, and in vivo occurrence. *Toxicol. Appl. Pharmacol.* 31, 325–351, 1975.
- Pelletier, P., Lavigne, D., Laroche, I., Cantin, F., Phillips, L., Fung, V., 2010. Additional properties studies of DNAN based melt-pour explosive formulations. In: *Insensitive Munitions and Energetics Materials Symposium 2010*. Munich, Germany.
- Rutkowski, J., Cirincione, R., Patel, C., 2010. Common low-cost insensitive munitions explosive to replace TNT and Comp B. In: *Insensitive Munitions and Energetics Materials Symposium 2010*. Munich, Germany.
- van der Schalie, W.H., 1985. The Toxicity of Nitroguanidine and Photolyzed Nitroguanidine to Freshwater Aquatic Organisms. Technical Report 8404. U.S. Army BRDL: Fort Detrick, Frederick, MD.
- Singh, G., Kapoor, I.P.S., Tiwari, S.K., Felix, P.S., 2001. Studies on energetic compounds: Part 16. Chemistry and decomposition mechanisms of 5-nitro-2,4-dihydro-3H-1,2,4-Triazole-3-One (NTO). *J. Hazard Mater.* 81 (1), 67–82.
- Smith, M.W., Cliff, M.D., 1999. NTO Based Explosive Formulations: A Technology Review; Technology Review DSTO-TR-0796. Weapons Systems Division Aeronautical and Maritime Research Laboratory, Salisbury South Australia.
- Spear, R.J., Louey, C.N., Wolfson, M.G., 1989. A Preliminary Assessment of 3-Nitro-1,2,4-triazol-5-one (NTO) as an Insensitive High Explosive. Defence Science and Technology Organisation. Materials Research Laboratory, Maribyrnong, Australia. Available online at: <http://www.dtic.mil/dtic/tr/fulltext/u2/a215063.pdf>. (Accessed 17 May 2017).
- Taylor, S., Hewitt, A., Lever, J., Hayes, C., Perovich, L., Thorne, P., Daghlia, C., 2004. TNT particle size distributions from detonated 155-mm howitzer rounds. *Chemosphere* 55, 357–367.
- Taylor, S., Dontsova, K., Walsh, M.E., Walsh, M.R., 2015a. Outdoor dissolution of three insensitive munitions formulations. *Chemosphere* 134, 250–256.
- Taylor, S., Park, E., Bullion, K., Dontsova, K., 2015b. Dissolution of three insensitive munitions formulations. *Chemosphere* 119, 342–348.
- Taylor, S., Dontsova, K., Walsh, M., 2017a. Insensitive munitions formulations: their dissolution and fate in soils. In: *Energetic Materials; Challenges and Advances in Computational Chemistry and Physics*. Springer, Cham, pp. 407–443.
- Taylor, S., Walsh, M.E., Becher, J.B., Ringelberg, D.B., Mannes, P.Z., Gribble, G.W., 2017b. Photo-degradation of 2,4-dinitroanisole (DNAN): an emerging munitions compound. *Chemosphere* 167, 193–203.
- Turovski, M., Deshmukh, B., 2004. Direct chromatographic method for determination of hydrogen cyanamide and dicyandiamide in aqueous solutions. *Anal. Lett.* 37 (9), 1981–1989.
- Urbanyi, T., Walter, A., 1971. IR determination of trace quantities of dicyandiamide and cyanamide in guanidine sulfate. *J. Pharm. Sci.* 60 (11), 1699–1701.
- U.S., 2014. Environmental Protection Agency Method 9014: Cyanide in Waters and Extracts Using Titrimetric and Manual Spectrophotometric Procedures; Test Methods for Evaluating Solid Waste: Physical/Chemical Methods. EPA Method SW-846 Update V.
- Walsh, M.R., Walsh, M.E., Ramsey, C.A., Taylor, S., Ringelberg, D., Zufelt, J., Thiboutot, S., Ampleman, G., Diaz, E., 2013. Characterization of PAX-21 insensitive munition detonation residues. *Propell. Explos. Pyrot.* 38, 399–409.
- Walsh, M.R., Walsh, M.E., Ramsey, C.A., Thiboutot, S., Ampleman, G., Diaz, E., Zufelt, J.E., 2014. Energetic residues from the detonation of IMX-104 insensitive munitions. *Propell. Explos. Pyrot.* 39, 243–250.
- Xue, Z., He, J., Zhang, J., Zhang, X., Chen, Y., Ren, F., 2017. Theoretical investigation of the safety of nitroguanidine-based PBXs containing the nonpolar desensitizing agent polytetrafluoroethylene. *J. Mol. Model.* 23 (12), 346.

# REPORT DOCUMENTATION PAGE

*Form Approved*  
OMB No. 0704-0188

Public reporting burden for this collection of information is estimated to average 1 hour per response, including the time for reviewing instructions, searching existing data sources, gathering and maintaining the data needed, and completing and reviewing this collection of information. Send comments regarding this burden estimate or any other aspect of this collection of information, including suggestions for reducing this burden to Department of Defense, Washington Headquarters Services, Directorate for Information Operations and Reports (0704-0188), 1215 Jefferson Davis Highway, Suite 1204, Arlington, VA 22202-4302. Respondents should be aware that notwithstanding any other provision of law, no person shall be subject to any penalty for failing to comply with a collection of information if it does not display a currently valid OMB control number. **PLEASE DO NOT RETURN YOUR FORM TO THE ABOVE ADDRESS.**

<b>1. REPORT DATE (DD-MM-YYYY)</b> August 2021		<b>2. REPORT TYPE</b> Final		<b>3. DATES COVERED (From - To)</b>	
<b>4. TITLE AND SUBTITLE</b>  Photo-transformation of Aqueous Nitroguanidine and 3-nitro-1,2,4-triazol-5-one: Emerging Munitions Compounds				<b>5a. CONTRACT NUMBER</b>	
				<b>5b. GRANT NUMBER</b>	
				<b>5c. PROGRAM ELEMENT NUMBER</b>	
<b>6. AUTHOR(S)</b>  Julie B. Becher, Samuel A. Beal, Susan Taylor, Katerina Dontsova, Dean E. Wilcox				<b>5d. PROJECT NUMBER</b>	
				<b>5e. TASK NUMBER</b>	
				<b>5f. WORK UNIT NUMBER</b>	
<b>7. PERFORMING ORGANIZATION NAME(S) AND ADDRESS(ES)</b>  See next page.				<b>8. PERFORMING ORGANIZATION REPORT NUMBER</b>  ERDC/CRREL MP-21-21	
				<b>10. SPONSOR/MONITOR'S ACRONYM(S)</b>  USACE	
<b>9. SPONSORING / MONITORING AGENCY NAME(S) AND ADDRESS(ES)</b> U.S. Army Corps of Engineers Washington, DC 20314				<b>11. SPONSOR/MONITOR'S REPORT NUMBER(S)</b>	
<b>12. DISTRIBUTION / AVAILABILITY STATEMENT</b>  Approved for public release; distribution is unlimited.					
<b>13. SUPPLEMENTARY NOTES</b> This article was originally published online in <i>Chemosphere</i> on 22 April 2019. Funding for this work was received from the USACE Engineer Research and Development Center and from the Department of Defense (DoD) Strategic Environmental Research and Development Program (SERDP), Project ER-2727. Ms. Becher received additional support from several programs at Dartmouth College.					
<b>14. ABSTRACT</b>  Two major components of insensitive munition formulations, nitroguanidine (NQ) and 3-nitro-1,2,4-triazol-5-one (NTO), are highly water soluble and therefore likely to photo-transform while in solution in the environment. The ecotoxicities of NQ and NTO solutions are known to increase with UV exposure, but a detailed accounting of aqueous degradation rates, products, and pathways under different exposure wavelengths is currently lacking. We irradiated aqueous solutions of NQ and NTO over a 32-h period at three ultraviolet wavelengths and analyzed their degradation rates and transformation products. NQ was completely degraded by 30 min at 254 nm and by 4 h at 300 nm, but it was only 10% degraded after 32 h at 350 nm. Mass recoveries of NQ and its transformation products were $\geq 80\%$ for all three wavelengths. NTO degradation was greatest at 300 nm with 3% remaining after 32 h, followed by 254 nm (7% remaining) and 350 nm (20% remaining). Mass recoveries of NTO and its transformation products were high for the first 8 h but decreased to 22–48% by 32 h. Environmental half-lives of NQ and NTO in pure water were estimated as 4 and 6 days, respectively. We propose photo-degradation pathways for NQ and NTO supported by observed and quantified degradation products and changes in solution pH.					
<b>15. SUBJECT TERMS</b>  UV irradiation, Nitroguanidine (NQ), 3-nitro-1,2,4-triazol-5-one (NTO), Transformation products, Transformation pathways					
<b>16. SECURITY CLASSIFICATION OF:</b>			<b>17. LIMITATION OF ABSTRACT</b>  UU	<b>18. NUMBER OF PAGES</b>  15	<b>19a. NAME OF RESPONSIBLE PERSON</b>
<b>a. REPORT</b>  Unclassified	<b>b. ABSTRACT</b>  Unclassified	<b>c. THIS PAGE</b>  Unclassified			<b>19b. TELEPHONE NUMBER (include area code)</b>

**7. PERFORMING ORGANIZATION NAME(S) AND ADDRESS(ES)**

*Environmental Laboratory  
U.S. Army Engineer Research and Development Center  
3992 Halls Ferry Road  
Vicksburg, MS 39180*

*Department of Chemistry  
Dartmouth College  
Hanover, NH 03755*

*Department of Soil, Water, and Environmental Science  
University of Arizona  
Tucson, AZ 85721*